Fulleropyrrolidines bearing π-conjugated moiety for polymer solar cells: contribution of the chromophoric substituent on C60 to photocurrent

ARTICLE *in* ACS APPLIED MATERIALS & INTERFACES · DECEMBER 2012

Impact Factor: 6.72

6 AUTHORS, INCLUDING:

S. P. Rwei
National Taipei University of Technology
83 PUBLICATIONS **692** CITATIONS

ACS APPLIED MATERIALS & INTERFACES

Research Article

www.acsami.org

[60]Fulleropyrrolidines Bearing π-Conjugated Moiety for Polymer Solar Cells: Contribution of the Chromophoric Substituent on C_{60} to the Photocurrent

Chinnusamy Saravanan,[†] Che-Liang Liu,[‡] Yi-Min Chang,[‡] Jan-De Lu,[§] Yen-Ju Hsieh,[‡] Syang-Peng Rwei,[§] and Leeyih Wang*[,†,‡]

[†]Centre for Condensed Matter Sciences, National Taiwan University, Taipei, Taiwan

[‡]Institute of Polymer Science and Engineering, National Taiwan University, Taiwan

[§]Institute of Organic and Polymeric Materials, National Taipei University of Technology, Taipei 106, Taiwan

Supporting Information

ABSTRACT: Two fullerene-terthiophene dyads without hexyl chains (3T-C_{60}) and with hexyl chains (3TH-C_{60}) on the terthiophene substituent are synthesized by 1,3-dipolar cycloaddition of corresponding azomethine ylides to C_{60}. The cyclic voltammetry studies indicate no apparent electronic communication between the terthiophene pendent group and the fulleropyrrolidine core in the ground state. However, a significant florescence quenching is observed for 3T-C_{60} and 3TH-C_{60}, compared to their fluorescent terthiophene (3T) and 3TH precursors, respectively, suggesting the occurrence of strong intramolecular electron/energy transfers in the photoexcited state. Furthermore, these new fulleropyrrolidine derivatives are applied as electron acceptors to fabricate poly(3-hexylthiophene) (P3HT) based bulk heterojunction solar cells. The incident photon-to-current efficiency (IPCE) value of the P3HT/3T-C_{60} device is significantly higher than that of the P3HT/PCBM cell in wavelengths of 350−420 nm. This finding provides direct evidence for the contribution of 3T excitons to the photocurrent. Replacing 3T-C_{60} with 3TH-C_{60} effectively improves the morphology of the photoactive layer and widens the window of optimal D/A ratios, raising the power conversion efficiency (PCE) from 2.14% to 2.54%. Importantly, these devices exhibit superior stability of PCE against high-temperature aging.

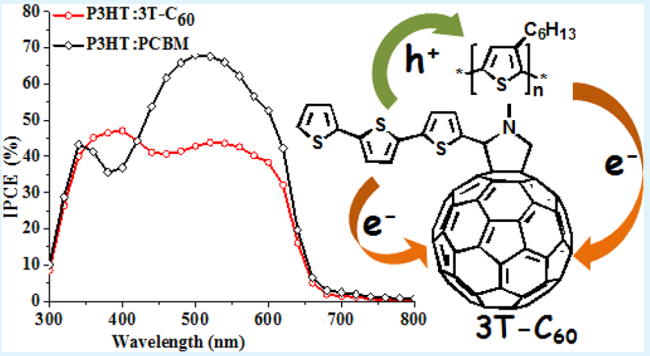

KEYWORDS: *fulleropyrrolidines, C_{60}, electron acceptor, polymer solar cells, morphology, thermal stability*

INTRODUCTION

With the potential of providing a low-cost and lightweight renewable energy source, organic photovoltaics have attracted considerable research interest in recent years.[1] The active layer in this type of solar cell is usually a binary blend of two compounds: one has a higher-lying lowest unoccupied molecular orbital (LUMO), acting as an electron donor (D), and the other acts as an electron acceptor (A). Because the excitons generated in organic materials typically have large binding energy and can only be efficiently dissociated into free carriers at the D/A interface with the aid of the energetic driving force originating from the differences in the electronic levels of the materials. Since Heeger et al.[2] discovered that C_{60} is an effective fluorescence quencher of conjugated polymer, fullerenes[3] and their derivatives[4] have been extensively used as acceptor materials in fabricating polymer solar cells. In particular, the [6,6]-phenyl-C_{61}-butyric acid methyl ester (PCBM) has become a benchmark acceptor. However, several drawbacks are associated with PCBM. Its high crystallinity causes the intermolecular aggregation of PCBMs into big particles inside a polymer matrix for the duration of coating and/or thermal aging, leading to an unfavorable morphology of the polymer/PCBM blends, thus lowering the environmental stability of solar devices, and complicating cell fabrication procedures.[5] In addition, the PCBM's relatively low-lying LUMO level frequently produces a large LUMO offset between itself and the polymer donor, such as poly(3-hexylthiophene) (P3HT), giving rise to a loss of a significant fraction of the photon energy during the photoinduced electron transfer process, thus causing a decline of the open-circuit voltage (V_{oc}).[6] Moreover, because of their low absorptivity in visible and near-infrared light regions, PCBM molecules barely create photoexcited excitons and, therefore, make little contribution to the photocurrent.[7] Especially, the light absorption range of

Received: August 24, 2012
Accepted: October 24, 2012
Published: October 24, 2012

   dx.doi.org/10.1021/am301773t | ACS Appl. Mater. Interfaces 2012, 4, 6133−6141

Scheme 1. Synthesis of 3T-C_{60}, 3TH-C_{60}, and NMP-C_{60}

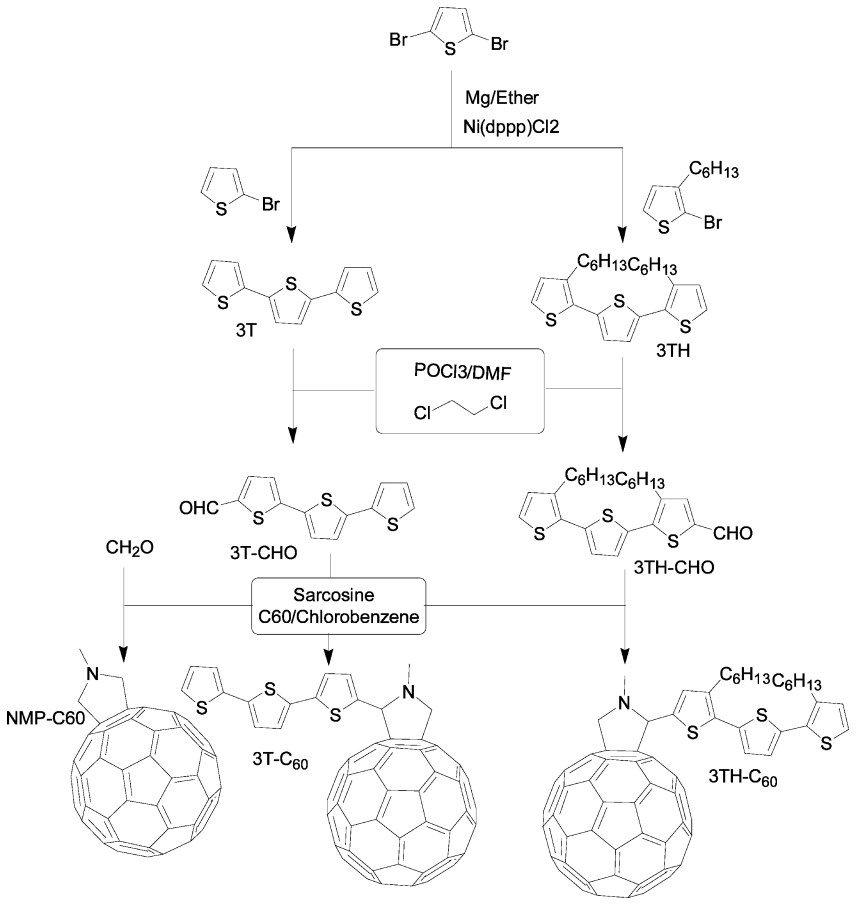

conjugated polymers is much narrower than the solar spectrum,[8] and the optimal thickness of the photoactive layer in devices is typically very thin (~100−200 nm).[9] These two factors limit the full utilization of the incident solar energy by plastic solar cells. Therefore, an obvious route to improve the efficiency of exciton generation is by employing a fullerene derivative with a high light-harvesting ability and a spectrum complementary to the polymer donor as an acceptor material in the active layer of solar cells.

Hummelen et al.[10] demonstrated that [6,6]-phenyl-C71-butyric acid methyl ester ($PC_{71}BM$) has an increased absorption in the visible region, compared to its C_{60} analogue, $PC_{61}BM$, because the asymmetric structure of the C_{70} cage allows the forbidden low-energy transitions in C_{60}. The substitution of $PC_{61}BM$ with $PC_{71}BM$ can generally increase the short-circuit current density (J_{sc}) and power conversion efficiency.[11] However, this molecule suffers from the high-cost, low-production yield and complicated procedures for isolating and purifying isomers. Previous studies on the photophysical properties of oligothiophene/fullerene dyads revealed that an energy transfer occurs between the oligothiophene chromophore and the fullerene core in a nonpolar solvent, but an efficient electron transfer occurs in a polar media and in solid state.[12] Numerous chromophores, including porphyrin,[13] phthalocyanine,[14] perylenediimides,[15] azobenzenes,[16] cyanovinylene-4-nitrophenyl,[17] and tetrathiafulvalene[18] have been covalently grafted onto C_{60} to form dyads. These molecules display enhanced light absorption ability and the presence of C_{60} can accelerate photoinduced intramolecular charge separation and retard charge recombination in some cases.[19] In addition, triads consisting of two fullerene cages and one chromophore have been designed and synthesized.[20] A high J_{sc} value can be obtained for solar devices using such fullerene derivatives as the acceptor.[17,21]

To investigate the contribution of the chromophore group of C_{60} adduct to the photocurrent while avoiding the interference of the polymer donor, the absorption spectrum of the π-conjugated substituent should be complementary to that of its polymer counterpart, with little overlap between the two spectra. Herein, we report the synthesis of two terthiophene-bearing C_{60} derivatives, namely 3T-C_{60} and 3TH-C_{60}, and blend them with P3HT to construct bulk heterojunction solar cells. Their chemical structures and preparation routes are shown in Scheme 1. Comparison between the IPCE spectra of the P3HT/3T-C_{60} and the P3HT/PCBM devices clearly indicates the involvement of the terthiophene unit in the generation of photocurrent in the wavelength region of 350−420 nm. Furthermore, the stability of both the blend morphology of P3HT/3TH-C_{60} and the cell performance of the device fabricated from such a blend are examined.

EXPERIMENTAL SECTION

Materials. Thiophene, 3-bromothiophene, 1-bromohexane, $POCl_3$, and *N*-bromosuccinimide (NBS) were purchased from Aldrich Chemicals and used without further purification. Poly(3,4-ethylenedioxythiophene):poly(styrenesulfonate) (PEDOT:PSS) (Baytron P VPAI 4083) was used as-received. Phenyl-C_{61}-butyric acid methyl ester ($PC_{61}BM$) and C_{60} were obtained from Nano-C, Inc. Poly(3-hexylthiophene) (P3HT) was prepared following the Grignard metathesis approach in our laboratory. Its head-to-tail regioregularity

was determined by the ^{1}H NMR method to be >98%. The number-average molecular weight is 45k g/mol and the polydispersity index is 1.2, based on GPC analysis (THF eluent, polystyrene standard).

SYNTHESIS OF FULLERENE-TERTHIOPHENE DYADS

Synthesis of 2,2′:5′,2″-Terthiophene (3T). 2-Bromothiophene (4.89 g, 30 mmol) was added dropwise under nitrogen into the suspension of Mg turnings (0.95 g, 39.2 mmol) in dry ether (40 mL), and the reaction mixture was allowed to stir until the complete disappearance of Mg turnings. This solution then was transferred slowly into a cooled mixture of 2,5-dibromothiophene (3.00 g, 12.4 mmol) and Ni(dppp)-Cl_2 (100 mg, 0.18 mmol) in dry ether (30 mL) through cannula. The reaction mixture was allowed to stir for another 16 h at room temperature, subsequently poured into ice/water (150 mL), and neutralized with concentrated HCl. The product was extracted with excess ether and washed with large amount of water and brine, successively. The organic extracts were dried over anhydrous $MgSO_4$, evaporated, and purified with column chromatography using silica gel to give 3T as a light-yellow solid with a yield of 79%. ^{1}H NMR (400 MHz, $CDCl_3$, δ, ppm): 7.19 (dd, 2H), 7.15 (dd, 2H) 7.06 (s, 1H), 6.99 (t, 2H). ^{13}C NMR (100 MHz, $CDCl_3$, δ, ppm): 137.12, 135.20, 127.85, 124.46, 124.29, 123.68.

Synthesis of 3,3″-Dihexyl-2,2′:5′,2″-terthiophene (3TH). The 3TH was synthesized with a yield of 64% by adopting the similar procedure for 3T but replacing 2-bromothiophene with 2-bromo-3-hexylthiophene as the reactant. ^{1}H NMR (400 MHz, $CDCl_3$, δ, ppm): 7.21 (d, 2H, Ar), 7.09 (s, 2H, Ar), 6.98 (d, 2H, Ar), 2.82 (t, 4H, Ar−$\underline{CH_2}$−CH_2−), 1.71−0.91 (m, 22H, aliphatic). ^{13}C NMR (100 MHz, $CDCl_3$, δ, ppm): 139.72, 136.09, 130.07, 126.08, 123.76, 31.72, 30.76, 29.34, 29.28, 22.67, 14.12.

Synthesis of 5-Formyl-2,2′:5′,2″-terthiophene (3T-CHO). A solution of 3T (1.00 g, 4.03 mmol) in dichloroethane (7 mL) was introduced into a round-bottom flask comprising phosphoryl chloride (0.59 g, 3.86 mmol), dry DMF (0.3 mL, 3.86 mmol) and dichloroethane (15 mL). After stirring overnight at room temperature, the reaction mixture was added with 1 M sodium acetate (30 mL), and then stirred for ∼8 h. The resulting solution was extracted with CH_2Cl_2, and the combined organic layer was washed with water, brine, sequentially, and dried over anhydrous $MgSO_4$. The crude product was finally purified by column chromatography to give the 3T-CHO as an orange solid with a yield of 81%. ^{1}H NMR (400 MHz, $CDCl_3$, δ, ppm): 9.84 (s, 1H, −CHO), 7.65 (d, 1H, Ar), 7.26−7.11 (m, 4H, Ar), 7.11 (d, 1H, Ar), 7.02 (d. 1H. Ar). ^{13}C NMR (100 MHz, $CDCl_3$, δ, ppm): 182.39, 146.82, 141.62, 139.18, 137.31, 136.42, 134.49, 128.06, 126.88, 125.39, 124.66, 124.50, 124.03.

Synthesis of 5-Formyl-3,3″-dihexyl-2,2′:5′,2″-terthiophene (3TH-CHO). The 3TH-CHO was synthesized with a yield of 75% by adopting the similar procedure for 3T-CHO but replacing 3T with 3TH as the reactant. ^{1}H NMR (400 MHz, $CDCl_3$, δ, ppm): 9.85 (s, 1H, −CHO), 7.61 (s, 1H, Ar), 7.25, (d, 1H, Ar), 7.24, (d, 1H, Ar), 7.11 (d, 1H, Ar), 6.98 (d, 1H, Ar), 2.86−2.79 (m, 4H, Ar−$\underline{CH_2}$−CH_2−), 1.75−0.92 (m, 22H, aliphatic). ^{13}C NMR (100 MHz, $CDCl_3$, δ, ppm): 182.50, 141.13, 140.36, 140.29, 140.22, 139.04, 138.51, 134.47, 130.24, 129.78, 127.77, 126.30, 124.40, 31.69, 31.64, 30.62, 30.30, 29.47, 29.26, 29.18, 14.03.

Synthesis of 2,2′:5′,2″-Terthiophene:fullerene dyad (3T-C_{60}). A mixture of 3T-CHO (128 mg, 0.046 mmol), C_{60} (100 mg, 0.139 mmol), and sarcosine (6.1 mg, 0.069 mmol) was dissolved in chlorobenzene (50 mL) and heated to 120 °C for 24 h. After cooling the reaction mixture to room temperature, the solvent was removed by an evaporator and the crude product was purified by column chromatography, using hexane/toluene (75/25 v/v) as an eluent to generate the dyad as a black solid with a yield of 45%. ^{1}H NMR (400 MHz, $CDCl_3$, δ, ppm): 7.30−6.97 (m, 7H, Ar), 5.20 (s, 1H, Pyro.), 4.96 (d, 1H, Pyro.), 4.23 (d, 1H, Pyro.) 2.91 (s, 3H, N−CH_3). MALDI-TOF MS: m/z 1024.15 (100%, $[M+H]^+$).

Synthesis of 3,3″-Dihexyl-2,2′:5′,2″-terthiophene:fullerene Dyad (3TH-C_{60}). The 3TH-C_{60} was also synthesized with a yield of 46% by adopting the similar procedure for 3T-C_{60} but replacing 3T-CHO with 3TH-CHO as the reactant. ^{1}H NMR (400 MHz, $CDCl_3$, δ, ppm): 7.26−6.95 (m, 5H, Ar), 5.19 (s, 1H, Pyro.), 5.01 (d, 1H, Pyro.), 4.27 (d, 1H, Pyro.) 2.98 (s, 3H, N−CH_3), 2.80 (s, (broad), 4H, Ar−$\underline{CH_2}$−CH_2−), 1.63−0.84 (m, 22H, aliphatic).

INSTRUMENTATION

^{1}H and ^{13}C NMR spectra were recorded on a Bruker Spectrospin-400 MHz spectrometer at room temperature using $CDCl_3$ as the solvent, and the solvent signal was adopted as an internal standard. The UV−vis and fluorescence spectra were measured using a Jasco-V660 spectrophotometer and Jobin−Yvon Fluorolog-TAU-3 spectrofluorimeter, respectively. Film thicknesses were determined using a Veeco α-step analyzer. Cyclic voltammetry (CV) measurements were performed with a 273A potentiostat from CH Instruments, which is equipped with a platinum disk as the working electrode, a platinum wire as the counter electrode, and a Ag/AgCl as the reference electrode, at a scan rate of 100 mV s^{-1} using o-dichlorobenzene/acetonitrile (o-DCB/AcCN) (4:1 v/v) and 0.1 M tetrabutylammonium hexafluorophosphate as the solvent and electrolyte, respectively. The reference electrode was calibrated with an internal standard of ferrocene. Transmission electron microscopy (TEM) and atomic force microscopy (AFM) images were captured using a Hitachi H-7100 microscope and a Digital Instruments Nano Scope IIIa atomic force microscope, respectively.

FABRICATION AND MEASUREMENT OF POLYMER SOLAR CELL

The polymer solar cells (PSCs) were fabricated in a configuration of the traditional sandwich structure with an indium tin oxide (ITO) glass as anode and a metal as cathode. The ITO glasses were cleaned by a sequential ultrasonic treatment in detergent, deionized water, acetone, and isopropanol for 20 min. Then PEDOT:PSS was filtered through a 0.2-μm filter and spin-coated at 3500 rpm for 30 s on top of ITO electrode. Subsequently, the PEDOT:PSS film was baked at 140 °C for 10 min in the air, and then moved into a glovebox. The blend solution of P3HT and synthesized dyads (3T-C_{60} and 3TH-C_{60}) in a cosolvent of o-DCB/TCB was filtered through a 0.45-μm filter and spin-coated at 800 rpm for 30 s on top of the PEDOT:PSS layer. These devices were thermally annealed at various temperatures for 10 min, followed by capping with Ca (∼20 nm) and then Al (∼60 nm) in a thermal evaporator at a base pressure of ca. 10^{-6} Pa. The active area of the devices is 0.06 cm^2. The current density−voltage

(J–V) measurements of the devices were conducted on a computer-controlled Keithley 2400 Source Measure Unit under AM1.5G simulated solar irradiation at 100 mW cm^{-2}. The light incident intensity was calibrated by a mono-Si reference cell with a KG5 filter (PV Measurements, Inc.), which was precalibrated by the National Renewable Energy Laboratory.

RESULTS AND DISCUSSION

Synthesis of Fullerene–Terthiophene Dyads. Scheme 1 depicts the synthetic routes for *N*-methyl fulleropyrrolidine (NMP-C_{60}) and its terthiophene-substituted derivatives, 3T-C_{60} and 3TH-C_{60}. 3T and 3TH were prepared by a nickel-catalyzed Kumada coupling reaction of 2,5-dibromothiophene with two equivalents of 2-bromothiophene and 2-bromo-3-hexylthiophene, respectively. These were then formylated using the Vilsmeier–Haack reaction, followed by the Prato reaction with C_{60} in the presence of sarcosine to produce 3T-C_{60} and 3TH-C_{60} with yields of 40% and 46%, respectively. Both the dyads exhibit adequate solubility in common organic solvents, such as chloroform, toluene, chlorobenzene (CB), and *o*-DCB. As expected, 3TH-C_{60} has higher solubility than 3T-C_{60} in *o*-DCB, because of the presence of two flexible hexyl chains on the terthiophene unit. Besides, the NMP-C_{60} was also synthesized by the 1,3-dipolar cycloaddition of C_{60} with an azomethine ylide, which is the reaction product of sarcosine and paraformaldehyde. The structure of all synthesized dyads was confirmed by the ^{1}H NMR and ^{13}C NMR spectra, elemental analysis, and mass spectral data.

Electrochemical and Optical Properties. The electrochemical behavior of 3T-C_{60} and 3TH-C_{60} was examined by cyclic voltammetry (CV) using *o*-DCB/MeCN (4:1 v/v) and 0.1 M Bu_4NPF_6 as the solvent and supporting electrolyte, respectively. Cyclic voltammograms of both fulleropyrrolidines in Figure 1 display three well-defined and reversible redox

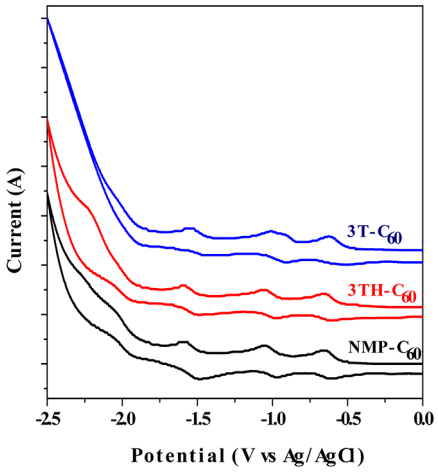

Figure 1. Cyclic voltammograms of 3T-C_{60}, 3TH-C_{60}, and NMP-C_{60} in a mixed solvent of *o*-DCB/ACN (4:1 v/v) with 0.1 M $TBAPF_6$ at a scan rate of 100 mV/s.

waves in the negative potential ranging from 0 to −2.5 V vs Ag/AgCl, suggesting excellent electrochemical stability of 3T-C_{60} and 3TH-C_{60} as electron acceptors. To explore the electronic effects exerted by the π-conjugated substituents on the fullerene component, CV measurements were also conducted for NMP-C_{60}. As observed in Figure 1, 3T-C_{60} and 3TH-C_{60} exhibit reduction behavior similar to NMP-C_{60}, demonstrating a weak electronic interaction between 3T and C_{60} in the ground state. Similar results have also been reported for many fullerene–chromophore dyads.[22] The energy levels of active components in solar devices are crucial to the efficient generation and dissociation of excitons. Hence, the LUMO value of the three fullerene compounds was determined from their first reduction potentials (E^{1}_{red}), based on the reference energy level of ferrocence ($E_{(Fc/Fc+)}$), which is −4.8 V below the vacuum level, according to the equation[23]

$$E_{LUMO}\ (eV) = -\left[E^{1}_{red} - E_{(Fc/Fc^{+})} + 4.8\right]$$

and they are found to have almost same LUMO value, of approximately −3.65 eV, which is comparable to the LUMO of PCBM (−3.67 eV). The HOMO and LUMO values of 3T and 3TH were calculated following the formulas of

$$E_{HOMO}\ (eV) = -\left[E^{1}_{ox} - E_{(Fc/Fc^{+})} + 4.8\right]$$

and

$$E_{LUMO} = E_g - E_{HOMO}$$

where E^{1}_{ox} is the first oxidation potential in their cyclic voltammograms (see Figures 1S and 2S in the Supporting Information) and E_g is the optical band gap, which was determined from the onset wavelength of the absorption bands of 3T and 3TH.

Applying the donor/acceptor blend, which has a high light-harvesting ability and broad absorption spectrum as the photoactive material of OPVs is essential in enhancing the J_{sc} value of solar devices. Figure 2 shows the UV–vis absorption

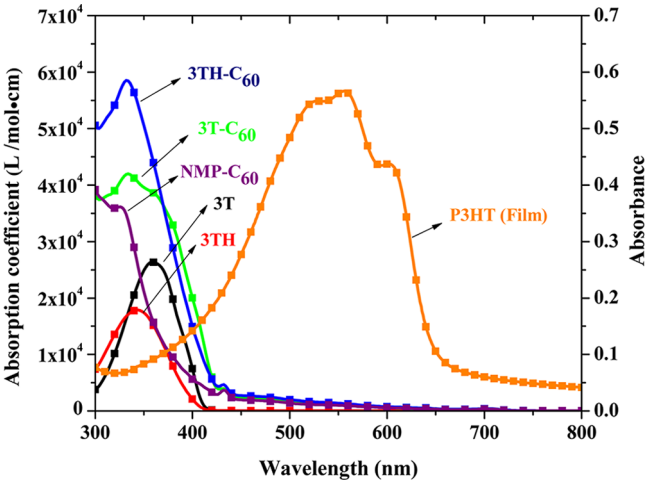

Figure 2. UV–vis absorption spectra of 3T, 3TH, NMP-C_{60}, 3T-C_{60} and 3TH-C_{60} in *o*-DCB and a thin film of P3HT.

spectra of 3T, 3TH, 3T-C_{60}, and 3TH-C_{60} in *o*-DCB and P3HT in thin film. Both 3T and 3TH exhibit single absorption peaks at 358 and 342 nm, respectively, corresponding to the π–π^* transition of the terthiophene unit. The presence of two hexyl chains blue-shifts the absorption maximum by 16 nm and reduces the molar absorptivity of the terthiophene. This is probably due to the steric hindrance of the two alkyl groups, which reduces the coplanarity of the three thiophenes and, thus, the degree of delocalization of π-electrons across rings.[24] Binding these two conjugates onto C_{60} through the Prato reaction generates characteristic peaks at 432 and 704 nm. Basically, both 3T-C_{60} and 3TH-C_{60} exhibit the combined

dx.doi.org/10.1021/am301773t | ACS Appl. Mater. Interfaces 2012, 4, 6133–6141

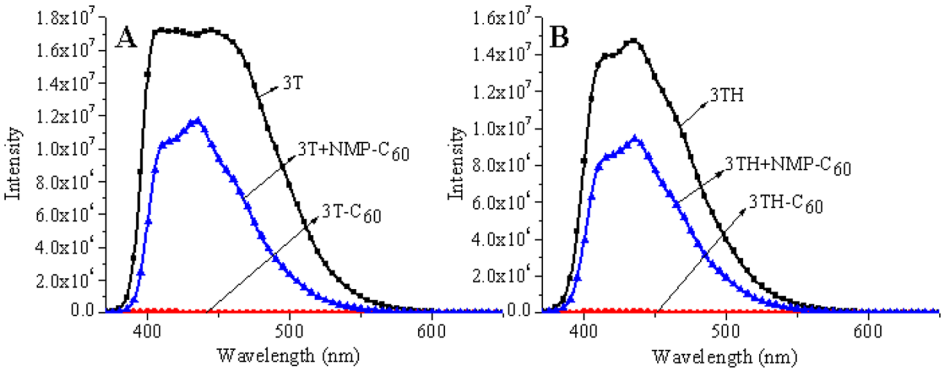

Figure 3. Fluorescence spectra of (A) 3T, 3T+NMP-C_{60}, and 3T-C_{60}; (B) 3TH, 3TH+NMP-C_{60}, and 3TH-C_{60} in *o*-DCB (2.7×10^{-5} M, excited at corresponding absorption maxima).

absorption features of C_{60} and the terthiophene components; 3T-C_{60} has a relatively broad absorption band with a maximum at 334 nm and a shoulder at 380 nm, and 3TH-C_{60} has sharp band with a maximum at 332 nm. These findings confirm that the C_{60} cage has no apparent effect on the energy levels of 3T substituents in the dyads, because of the disruption of conjugation between C_{60} and the terthiophene by the bridged groups. The presence of two hexyl chains effectively increases the solubility of 3TH-C_{60} in *o*-DCB and may hinder the $\pi-\pi$ stacking of C_{60} cages. Accordingly, the small hump at 380 nm in the absorption spectrum is reasonably attributed to molecular aggregates of 3T-C_{60}. The complementary feature of the absorption bands of 3T-C_{60} and 3TH-C_{60} with that of P3HT not only broadens the light-harvesting range of P3HT but also allows us to investigate whether the excitons generated in the conjugate substituent of fullerene acceptors can contribute to the photocurrent without complication by P3HT excitons.

As shown in Figure 3, the solution of 3T in *o*-DCB displays a broad photoluminescence (PL) spectrum with a plateau ranging from 400 nm to 480 nm upon photoexcitation at its absorption maximum. The addition of NMP-C_{60} as a co-solute slightly decreases the emission intensity of 3T to ~60% of its original value, because of the fact that the LUMO of NMP-C_{60} is lower-lying than that of 3T, providing a separate route to quench the excited electrons of 3T. Interestingly, the 3T-C_{60} solution exhibits a very weak PL intensity that demonstrates an efficient energy/electron transfer from the terthiophene unit to the C_{60} cage in the photoexcited state, and the covalent linkage between 3T and C_{60} shortens the physical distance between the two species, thereby enhancing the transfer efficiency. Similarly, the emission intensity of 3TH-C_{60} is much weaker than that of the mixed solution of 3TH and NMP-C_{60}. These observations suggest that the excitons generated in 3T may contribute to the photocurrent of the 3T-C_{60}- or 3TH-C_{60}-based solar devices.

Photovoltaic Properties. The new fulleropyrrolidine with conjugated substituent 3T-C_{60} was employed as the electron acceptor counterpart of the P3HT donor to fabricate solar cells with a configuration of ITO/PEDOT:PSS/P3HT:3T-C_{60}/Ca/Al. The film thickness of the active layer is ~100 nm. It is well-known that the blend ratio[25] of donor and acceptor materials in the active layer of BHJ solar cells plays an important role in determining the device's power conversion efficiency by altering the light-harvesting capability and morphology of the D/A blend, and the optimal ratio is a function of many factors, including the molecular structure of the materials, the compatibility of D and A, and the processing solvent.[26] A low content of fullerene derivative will result in the loss of the continuous paths for transporting electrons to the cathode that increases the number of charge carrier traps inside the photoactive layer; on the other hand, a low content of polymer donor will reduce the light-harvesting capability and may also lower the hole mobility of the photoactive blend. Figure 4

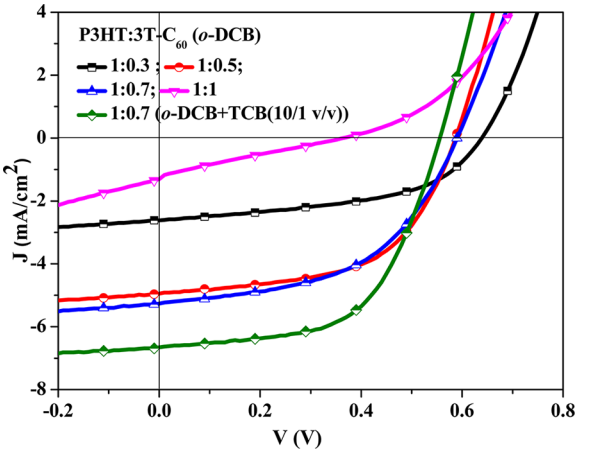

Figure 4. Current density–voltage ($J-V$) characteristics of the solar devices based on the blends of P3HT and 3T-C_{60} with various weight ratios of the two materials.

shows the current density–voltage ($J-V$) curves of the BHJ solar devices with various blend ratios of P3HT/3T-C_{60} measured under simulated one-sun AM1.5G illumination, and Table 1 summarizes their corresponding device parameters.

As the weight ratio of 3T-C_{60}/P3HT increases from 0.3 to 0.5, to 0.7, the photocurrent density rises from 2.62 mA cm^{-2}

Table 1. Photovoltaic Characteristics of the BHJ P3HT/3T-C_{60} Devices

weight ratio (P3HT:3T-C_{60})	solvent	open-circuit voltage, V_{oc} (V)	short-circuit current density, J_{sc} (mA cm^{-2})	FF (%)	PCE (%)
1: 0.3	*o*-DCB	0.64	2.62	50.16	0.84
1:0.5	*o*-DCB	0.59	4.95	55.95	1.63
1:0.7	*o*-DCB	0.60	5.27	50.17	1.59
1:1	*o*-DCB	0.37	1.31	21.54	0.10
1:0.7	(*o*-DCB/TCB)[a]	0.56	6.65	57.47	2.14

[a]The ratio of *o*-DCB/TCB is 10:1(v/v).

dx.doi.org/10.1021/am301773t | ACS Appl. Mater. Interfaces 2012, 4, 6133–6141

to 4.95 mA cm^{-2} to 5.27 mA cm^{-2}, while maintaining the V_{oc} value at ~0.6 V. However, further increasing the weight ratio to 1:1 significantly deteriorates all photovoltaic parameters (V_{oc}, J_{sc}, and FF) and results in a very low level of cell efficiency. This is mainly due to the limited solubility of 3T-C_{60} in organic solvent; the high concentration of 3T-C_{60} in the P3HT/3T-C_{60} (1:1 w/w) coating solution caused the precipitation of 3T-C_{60} as large clusters during the spin-drying process. These clusters degrade the paths along which electrons are transported to the cathode, thereby increasing the rate of recombination of carriers and reducing the open-circuit voltage. Several studies[27] have demonstrated that incorporating a small amount of a high-boiling-point liquid into the coating solution of the photoactive blend as processing additive can usually enhance the PCE of BHJ solar devices by inducing favorable phase separation of D/A materials and promoting the ordered packing of polymer chains. Figure 4 and Table 1 show that incorporating a small amount of TCB as the cosolvent of the photoactive blend increases the J_{sc} value by ~26%, to 6.65 mA cm^{-2}, at the expense of a slight decrement of V_{oc}, yielding a PCE value of 2.14%.

Scheme 2 depicts the energy level diagram of the P3HT/3T-C_{60} solar device based on the energy levels of active components determined in the CV and UV−vis experiments. Per the discussion in the section on electrochemical and optical properties, no apparent ground-state interactions are observed between the C_{60} core and 3T substituent in 3T-C_{60}, so both building blocks can be treated as independent molecules. Hence, the energy levels of NMP-C_{60} and 3T are presented, instead of 3T-C_{60}. There are three possible routes to generate free carriers in this system: the excitons generated in the P3HT, 3T substituent, and C_{60} cage may dissociate into electrons and holes at the interfaces of the three materials. Moreover, they are energetically favorable to inject the photoexcited electrons of the 3T moiety into the LUMO of the C_{60} monoadduct, and to reduce the 3T cations by P3HT. Although the 3T excitons can be dissociated at both interfaces of 3T/P3HT and 3T/C_{60}, the chemical bonding between 3T and C_{60} maintains the 3T moiety adjacent to the C_{60} cage, ensuring an efficient charge transfer between the two units. To examine the individual contribution of the P3HT donor and 3T-C_{60} acceptor in the generation of the solar device's photocurrent, the incident photon-to-current efficiency (IPCE) of an optimized P3HT/3T-C_{60} cell was measured across the entire visible spectral range and compared with that of a standard P3HT/PCBM cell. The integral of the IPCE of both devices over the AM 1.5G solar spectrum agrees well with the J_{sc} values observed in their $J-V$ curves. As displayed in Figure 5, the P3HT/3T-C_{60} device exhibits a very broad IPCE spectrum with plateau values of ~40%−45% in the wavelength range of 350−600 nm. Particularly, the P3HT/3T-C_{60} cell has higher IPCEs than those of the P3HT/PCBM cell between 350 nm and 420 nm. These findings demonstrate that the photoinduced excitons created in 3T-C_{60} can smoothly dissociate into free carriers and then contribute to photocurrent as P3HT excitons, and that binding appropriate color moieties onto fullerene acceptors is an effective approach to improving the sunlight absorption of its blends with polymer donor to produce more excitons. However, the IPCE of the P3HT/3T-C_{60} device is substantially lower than that of P3HT/PCBM device in the wavelength range of 420−650 nm, corresponding to the absorption range of P3HT. The relatively poor IPCE probably arises from the limited solubility of 3T-C_{60} (~15 mg mL^{-1}) in *o*-DCB, which causes the 3T-C_{60} may partially precipitate out of the coating solution and form large clusters within the P3HT matrix during the spin-drying process. These clusters result in an unfavorable morphology of the BHJ and a reduced efficiency of exciton dissociation.

Scheme 2. Schematic Diagram of the Energy Levels of Active Components in the P3HT/3T-C_{60} Solar Devices

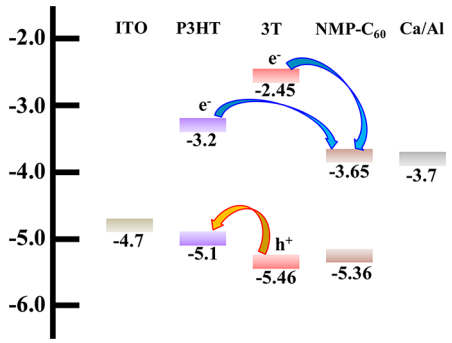

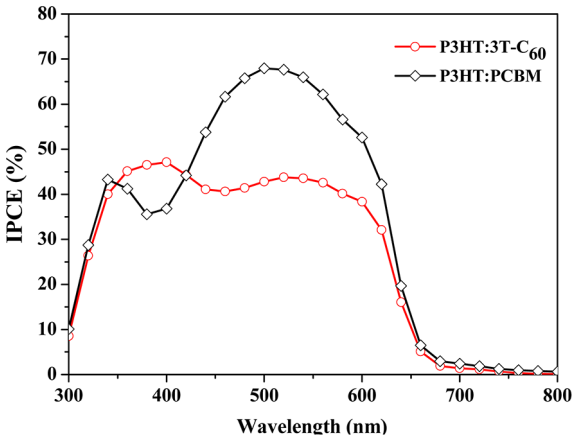

Figure 5. IPCE spectra of the P3HT/PCBM and P3HT/3T-C_{60} solar devices.

It has been demonstrated that the use of conjugated polymer and fullerene derivatives with comparable solubility as the respective donor and acceptor can raise the PCE of BHJ solar cells.[28] To achieve a better match with the solubilities of fulleropyrrolidine and P3HT, 3T-C_{60} was replaced with 3TH-C_{60}, which has flexible hexyl chains on both terminal thiophene rings of 3T, to fabricate solar cells using a *o*-DCB/TCB mixture (10:1, v/v) as processing solvent.

Figure 6 and Table 2 illustrate the photovoltaic performance of such devices at various P3HT/3TH-C_{60} ratios. This replacement results in an ~14% increment in J_{sc}; therefore, all P3HT/3TH-C_{60} devices herein have a better PCE than does the optimized P3HT/3T-C_{60} device. Numerous investigations[29] have demonstrated that the performance of polymer solar cells are critically dependent on the morphology of the active layer. To better understand the morphology of BHJ blends, the surfaces of the spin-coated films of P3HT/3T-C_{60} and P3HT/3TH-C_{60} on top of PEDOT:PSS were examined by a tapping-mode AFM system. Figure 7 indicates that the former is rougher than the latter, implying an improved miscibility between 3TH and P3HT that increases the interfacial area of D/A couples and the dissociation efficiency of excitons.

dx.doi.org/10.1021/am301773t | ACS Appl. Mater. Interfaces 2012, 4, 6133−6141

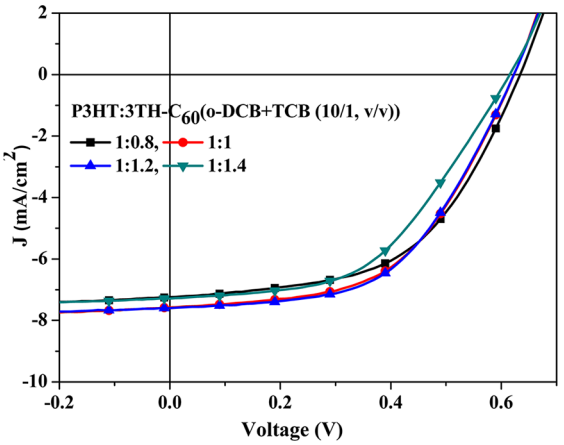

Figure 6. Current density–voltage (J–V) characteristics of the solar devices based on the blends of P3HT and 3TH-C_{60} with various weight ratios of the two materials.

Table 2. Photovoltaic Characteristics of the BHJ P3HT/3TH-C_{60} Devices

weight ratio (P3HT:3TH-C_{60})	solvent	open-circuit voltage, V_{oc} (V)	short-circuit current density, J_{sc} (mA/cm^2)	FF (%)	PCE (%)
1:0.8	*o*-DCB/TCB[a]	0.64	7.25	52.98	2.46
1:1	*o*-DCB/TCB[a]	0.63	7.58	52.78	2.52
1:1.2	*o*-DCB/TCB[a]	0.63	7.60	53.09	2.54
1:1.4	*o*-DCB/TCB[a]	0.62	7.28	49.52	2.24

[a]The ratio of *o*-DCB/TCB is 10:1 (v/v).

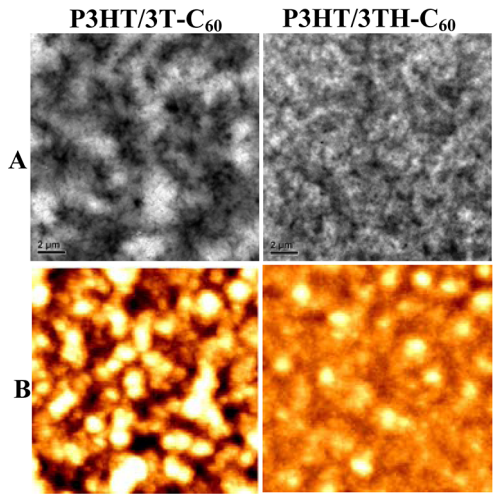

Figure 7. (A) TEM and (B) AFM images of the films of the P3HT/3T-C_{60} and P3HT/3TH-C_{60} blends, which were annealed at 140 °C for 10 min.

Moreover, the TEM images confirm that the domain size of the P3HT/3T-C_{60} is substantially larger than that of the P3HT/3TH-C_{60}. Interestingly, the variation of the weight ratio of P3HT/3TH-C_{60} (from 1:0.8 to 1:1.4) has no evident effect on the value of J_{sc}. These results suggest that incorporating alkyl groups into 3T-C_{60} not only improves the morphology of the polymer–fullerene BHJ blend but also widens the window of the optimal D/A ratio, thus simplifying cell fabrication conditions and enhancing device reproducibility. Although the best PCE of P3HT/3TH-C_{60} cell (2.54%) is somewhat lower than that (3.61%) of a standard P3HT/PCBM cell, it can be further improved by fine-tuning the solubility of the fullerene adduct and the miscibility of this molecule with the polymer donor.

Morphological Stability. The operational lifetime of a solar cell is one of decisive factors for its commercialization. However, aging a P3HT/PCBM blend under high temperatures usually leads to the formation of microscale phase domains, which notably reduces the interfacial area of the two materials and demolishes the continuous pathways of carriers to electrodes, thereby deteriorating cell efficiency. To study the morphological stability of the photoactive layer and its influence on cell performance, the polymer:fullerene blending films were heated at 130 °C for various durations prior to the deposition of the Ca/Al as cathode. Figure 8 shows that the

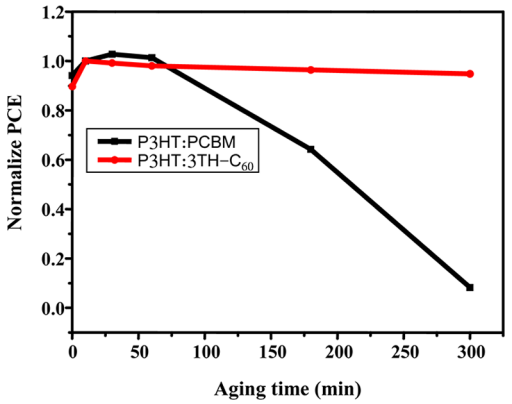

Figure 8. Plots of PCE versus the duration of thermal aging at 130 °C for the P3HT:3TH-C_{60} and P3HT: PCBM devices.

initial short-term heat treatment increases the PCEs for both devices, because of the formation of optimal blend morphology of the photoactive layer, as observed in many polymer-based BHJ systems. However, as reported elsewhere,[30] the PCE of the P3HT/PCBM device drops rapidly to less than one-tenth of its original value after high-temperature heating for 300 min. In contrast, the PCE of the P3HT/3TH-C_{60} device remains very steady during the course of thermal treatment and drops slightly by ~5% from its maximum value after 300 min of aging. Both OM and TEM were employed to explore the effect of high-temperature aging on the distribution and sizes of phase domains in polymer:fullerene blends. Figure 9 shows the as-spun P3HT/PCBM film has a smooth and homogeneous morphology; however, thermal aging induces the generation of numerous microsized clusters throughout the entire film. In contrast, the morphology of the P3HT/3TH-C_{60} blend remains steady after 5 h of thermal aging at 130 °C.

CONCLUSIONS

This work presents the synthesis of [60]fulleropyrrolidines bearing a terthiophene substituent via the Proto route. These dyads lack electronic communication between the 3T moiety and C_{60} cage in the ground state; therefore, they can be considered as independent units inside the photoactive layer of solar devices. Since the LUMO of 3T lies higher than the LUMO of NMP-C_{60} and its HOMO lies lower than that of P3HT, both the transfer of photoexcited electrons from 3T to

dx.doi.org/10.1021/am301773t | ACS Appl. Mater. Interfaces 2012, 4, 6133–6141

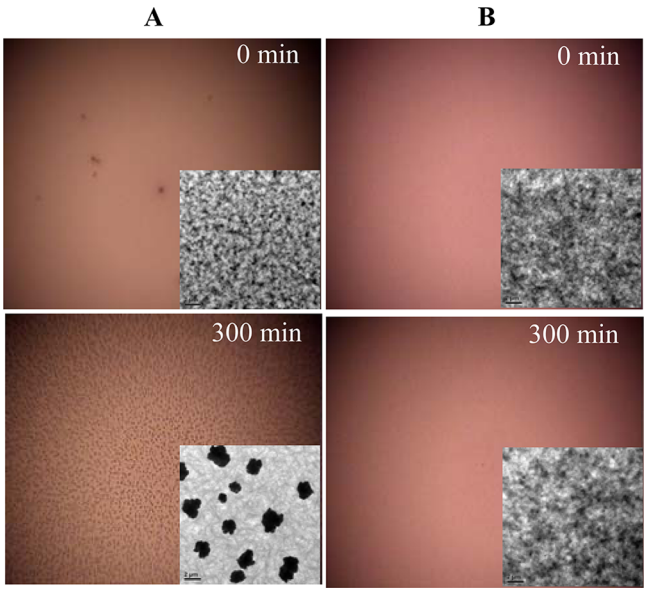

Figure 9. Optical microscope images of (A) P3HT/PCBM and (B) P3HT/3TH-C_{60} blend films before and after thermal aging at 130 °C for 300 min (the inset shows the TEM images of the corresponding blends).

C_{60} and the reduction of 3T cations are energetically feasible. Photoluminescence measurements reveal that 3T-C_{60} and 3TH-C_{60} exhibit strong electron/energy transfers between the two building components in the photoexcited state. Although the absorption of the 3T and 3TH moieties of [60]-fulleropyrrolidines is limited to the extreme blue end of the solar spectrum and contributes weakly to the production of excitons, the comparison of the IPCE spectrum of the P3HT/PCBM cell with that of the P3HT/3T-C_{60} device clearly demonstrates the excitons created in P3HT as well as 3T contribute to the photocurrent. This observation suggests that grafting a fullerene cage with color substituent, possessing suitable energy levels and a complementary light absorption spectrum, is a feasible approach to extend the light-harvesting wavelength range and increase the generation efficiency of excitons of the polymer:fullerene blends in polymer solar cells. Using 3TH-C_{60} to overcome the low solubility drawback of 3T-C_{60}, the P3HT/3TH-C_{60} device exhibits improved miscibility of D/A materials, thereby enhancing the J_{sc} value and PCE of the device. Further improvements of cell performance can be achieved by fine-tuning the solubility of fullerene−chromophore dyads and their compatibility with the polymer donor.

■ ASSOCIATED CONTENT

Ⓢ Supporting Information

Cyclic voltammograms of 3T and 3TH. This information is available free of charge via the Internet at http://pubs.acs.org.

■ AUTHOR INFORMATION

Corresponding Author

*Tel.: +886-2-3366-5276. Fax: +886-2-2365-5404. E-mail: leewang@ntu.edu.tw.

Notes

The authors declare no competing financial interest.

■ ACKNOWLEDGMENTS

The authors thank National Taiwan University, Academia Sinica, and the National Science Council of Taiwan, Republic of China (NSC 96-2113-M-002-012-MY3) for financially supporting this research.

■ REFERENCES

(1) (a) Gunes, S.; Neugebauer, H.; Sariciftci, N. S. *Chem. Rev.* **2007**, *107*, 1324. (b) Thompson, B. C.; Frechet, J. M. J. *Angew. Chem., Int. Ed.* **2008**, *47*, 58. (c) Brunetti, F. G.; Kumar, R.; Wudl, F. J. *J. Mater. Chem.* **2010**, *20*, 2934. (d) Topham, P. D.; Parnell, A. J.; Hiorns, R. C. *J. Polym. Sci., Part B: Polym. Phys.* **2011**, *49*, 1131.

(2) Yu, G.; Gao, J.; Hummelen, J. C.; Wudl, F.; Heeger, A. J. *Science* **1995**, *270*, 1789.

(3) (a) Brabec, C. J.; Sariciftci, N. S.; Hummelen, J. C. *Adv. Funct. Mater.* **2001**, *11*, 15. (b) Singh, Th. B.; Marjanović, N.; Matt, G. J.; Günes, S.; Sariciftci, N. S.; Ramil, A. M.; Andreev, A.; Sitter, H.; Schwödiauer, R.; Bauer, S. *Org. Electron.* **2005**, *6*, 105. (c) Chen, G.; Sasabe, H.; Wang, Z.; Wang, X.-F.; Hong, Z.; Yang, Y.; Kido, J. *Adv. Mater.* **2012**, *24*, 2768.

(4) (a) Varotto, A.; Treat, N. D.; Jo, J.; Shuttle, C. G.; Batara, N. A.; Brunetti, F. G.; Seo, J. H.; Chabinyc, M. L.; Hawker, C. J.; Heeger, A. J.; Wudl, F. *Angew. Chem., Int. Ed.* **2011**, *50*, 5166. (b) Chang, C.-Y.; Wu, C.-E.; Chen, S.-Y.; Cui, C.; Cheng, Y.-J.; Hsu, C.-S.; Wang, Y.-L.; Li, Y. *Angew. Chem., Int. Ed.* **2011**, *50*, 9386. (c) Wei, Q.; Nishizawa, T.; Tajima, K.; Hashimoto, K. *Adv. Mater.* **2008**, *20*, 2211. (d) He, Y.; Chen, H-Yu.; Hou, J.; Li, Y. *J. Am. Chem. Soc.* **2010**, *132*, 1377. (e) Ross, R. B.; Cardona, C. M.; Guldi, D. M.; Sankaranarayanan, S. G.; Reese, M. O.; Kopidakis, N.; Peet, J.; Walker, B.; Bazan, G. C.; Keuren, E. V.; Holloway, B. C.; Drees, M. *Nat. Matter* **2009**, *8*, 208. (f) Cheng, Y.-J.; Liao, M.-H.; Chang, C.-Y.; Kao, W.-S.; Wu, C.-E.; Hsu, C.-S. *Chem. Mater.* **2011**, *23*, 4056. (g) Kim, K.-H.; Kang, H.; Nam, S. Y.; Jung, J.; Kim, P. S.; Cho, C.-H.; Lee, C.; Yoon, S. C.; Kim, B. J. *Chem. Mater.* **2011**, *23*, 5090.

(5) Zhang, Y.; Yip, H.-L.; Acton, O.; Hau, S. K.; Huang, F.; Jen, A. K.-Y. *Chem. Mater.* **2009**, *21*, 2598.

(6) Koster, L. J. A.; Mihailetchi, V. D.; Blom, P. W. M. *Appl. Phys. Lett.* **2006**, *88*, 093511.

(7) (a) Cook, S.; Ohkita, H.; Kim, Y.; Benson-Smith, J. J.; Bradley, D. D. C.; Durrant, J. R. *Chem. Phys. Lett.* **2007**, *445*, 276. (b) Nicolaidis, N. C.; Routley, B. S.; Holdsworth, J. L.; Belcher, W. J.; Zhou, X.; Dastoor, P. C. *J. Phys. Chem. C* **2011**, *115*, 7801.

(8) (a) Beaujuge, P. M.; Amb, C. M.; Reynolds, J. R. *Acc. Chem. Res.* **2010**, *43*, 1396. (b) Wu, J.-S.; Cheng, Y.-J.; Dubosc, M.; Hsieh, C.-H.; Chang, C.-Y.; Hsu, C.-S. *Chem. Commun.* **2010**, *46*, 3259. (c) Ahmed, E.; Subramaniyan, S.; Kim, F. S.; Xin, H.; Jenekhe, S. A. *Macromolecules* **2011**, *44*, 7207. (d) Peng, Q.; Liu, X.; Qin, Y.; Xu, J.; Li, M.; Dai, L. *J. Mater. Chem.* **2011**, *21*, 7714.

(9) Renz, J. A.; Keller, T.; Schneider, M.; Shokhovets, S.; Jandt, K. D.; Gobsch, G.; Hoppe, H. *Sol. Energy Mater. Sol. Cells* **2009**, *93*, 508.

(10) Wienk, M. M.; Kroon, J. M.; Verhees, W. J. H.; Knol, J.; Hummelen, J. C.; Van Hal, P. A.; Janssen, R. A. J. *Angew. Chem., Int. Ed.* **2003**, *42*, 3371.

(11) Chen, H.-Y.; Wu, J.-L.; Chen, C.-T.; Chen, C.-T. *Chem. Commun.* **2012**, *48*, 1012.

(12) (a) Yamashiro, T.; Aso, Y.; Otsubo, T.; Tang, H.; Harima, Y.; Yamashita, K. *Chem. Lett.* **1999**, 443. (b) Fujitsuka, M.; Ito, O.; Yamashiro, T.; Aso, Y.; Otsubo, T. *J. Phys. Chem. A* **2000**, *104*, 4876. (c) Fujitsuka, M.; Masuhara, A.; Kasai, H.; Oikawa, H.; Nakanishi, H.; Ito, O.; Yamashiro, T.; Aso, Y.; Otsubo, T. *J. Phys. Chem. B* **2001**, *105*, 9930.

(13) (a) Chukharev, V.; Tkachenko, N. V.; Efimov, A.; Guldi, D. M.; Hirsch, A.; Scheloske, M.; Lemmetyinen, H. *J. Phys. Chem. B* **2004**, *108*, 16377.

(14) Bottari, G.; Olea, D.; Gómez-Navarro, C.; Zamora, F.; Gómez-Herrero, J.; Torres, T. *Angew. Chem., Int. Ed.* **2008**, *47*, 2026.

(15) Chamberlain, T. W.; Davies, E. S.; Khlobystov, A. N.; Champness, N. R. *Chem.—Eur. J.* **2011**, *17*, 3759.

(16) (a) Wang, M.; Chesnut, E.; Sun, Y.; Tong, M.; Guide, M.; Zhang, Y.; Treat, N. D.; Varotto, A.; Mayer, A.; Chabinyc, M. L.; Nguyen, T.-Q.; Wudl, F. *J. Phys. Chem. C* **2012**, *116*, 1313. (b) Schuster, D. I.; Li, K.; Guldi, D. M.; Palkar, A.; Echegoyen, L.; Stanisky, C.; Cross, R. J.; Niemi, M.; Tkachenko, N. V.; Lemmetyinen, H. *J. Am. Chem. Soc.* **2007**, *129*, 15973.
(17) (a) Mikroyannidis, J. A.; Kabanakis, A. N.; Sharma, S. S.; Sharma, G. D. *Adv. Funct. Mater.* **2011**, *21*, 746. (b) Mikroyannidis, J. A.; Tsagkournos, D. V.; Sharma, S. S.; Sharma, G. D. *J. Phys. Chem. C* **2011**, *115*, 7806.
(18) (a) Sánchez, L.; Sierra, M.; Martín, N.; Guldi, D. M.; Wienk, M. W.; Janssen, R. A. J. *Org. Lett.* **2005**, *7*, 1691. (b) Baffreau, J.; Dumur, F.; Hudhomme, P. *Org. Lett.* **2006**, *8*, 1307.
(19) Sandanayaka, A. S. D.; Taguri, Y.; Araki, Y.; Ishi-i, T.; Mataka, S.; Ito, O. *J. Phys. Chem. B* **2005**, *109*, 22502.
(20) (a) Shirai, Y.; Zhao, Y.; Cheng, L.; Tour, J. M. *Org. Lett.* **2004**, *6*, 2129. (b) Sánchez, L.; Herranz, M.; Martín, N. *J. Mater. Chem.* **2005**, *15*, 1409. (c) Atienza, C.; Insuasty, B.; Seoane, C.; Martín, N.; Ramey, J.; Rahmand, G. M. A.; Guldi, D. M. *J. Mater. Chem.* **2005**, *15*, 124.
(21) Wang, C.-L.; Zhang, W.-B.; Van Horn, R. M.; Tu, Y.; Gong, X.; Cheng, S. Z. D.; Sun, Y.; Tong, M.; Seo, J.; Hsu, B. B. Y.; Heeger, A. J. *Adv. Mater.* **2011**, *23*, 2951.
(22) (a) Sandanayaka, A. S. D.; Matsukawa, K.; Ishi-i, T.; Mataka, S.; Araki, Y.; Ito, O. *J. Phys. Chem. B* **2004**, *108*, 19995. (b) Narutaki, M.; Takimiya, K.; Otsubo, T.; Harima, Y.; Zhang, H.; Araki, Y.; Ito, O. *J. Org. Chem.* **2006**, *71*, 1761.
(23) Al-Ibrahim, M.; Roth, H.-K.; Schroedner, M.; Konkin, A.; Zhokhavets, U.; Gobsch, G.; Scharff, P.; Sensfuss, S. *Org. Electron.* **2005**, *6*, 65.
(24) (a) Darling, S. B. *J. Phys. Chem. B* **2008**, *112*, 8891. (b) Darling, S. B.; Sternberg, M. *J. Phys. Chem. B* **2009**, *113*, 6215.
(25) (a) Van Bavel, S. S.; Bärenklau, M.; De With, G.; Hoppe, H.; Loos, J. *Adv. Funct. Mater.* **2010**, *20*, 1458−1463. (b) Kwon, M. H. *Trans. Electr. Electron. Mater.* **2012**, *13*, 98. (c) Khlyabich, P. P.; Burkhart, B.; Thompson, B. C. *J. Am. Chem. Soc.* **2011**, *133*, 14534.
(26) (a) Brabec, C. J.; Heeney, M.; McCulloch, I.; Nelson, J. *Chem. Soc. Rev.* **2011**, *40*, 1185. (b) Thompson, B. C.; Fréchet, J. M. J. *Angew. Chem., Int. Ed.* **2008**, *47*, 58.
(27) (a) Salim, T.; Wong, L. H.; Bräuer, B.; Kukreja, R.; Foo, Y. L.; Bao, Z.; Lam, Y. M. *J. Mater. Chem.* **2011**, *21*, 242. (b) Jeong, S.; Kwon, Y.; Choi, B.-D.; Kwak, G.; Han, Y. S. *Macromol. Chem. Phys.* **2010**, *211*, 2474. (c) Xin, H.; Guo, X.; Ren, G.; Watson, M. D.; Jenekhe, S. A. *Adv. Energy Mater.* **2012**, *2*, 575. (d) Lee, J. K.; Ma, W. L.; Brabec, C. J.; Yuen, J.; Moon, J. S.; Kim, J. Y.; Lee, K.; Bazan, G. C.; Heeger, A. J. *J. Am. Chem. Soc.* **2008**, *130*, 3619. (e) Peet, J.; Cho, N. S.; Lee, S. K.; Bazan, G. C. *Macromolecules* **2008**, *41*, 8655.
(28) Troshin, P. A.; Hoppe, H.; Renz, J.; Egginger, M.; Mayorova, J. Y.; Goryachev, A. E.; Peregudov, A. S.; Lyubovskaya, R. N.; Gobsch, G.; Sariciftci, N. S.; Razumov, V. F. *Adv. Funct. Mater.* **2009**, *19*, 779.
(29) (a) Chen, W.; Nikiforov, M. P.; Darling, S. B. *Energy Environ. Sci.* **2012**, *5*, 8045. (b) Liu, F.; Gu, Y.; Jung, J. W.; Jo, W. H.; Russell, T. P. *J. Polym. Sci. Polym. Phys.* **2012**, *50*, 1018.
(30) (a) Meng, X.; Zhang, W.; Tan, Z.; Li, Y.; Ma, Y.; Wang, T.; Jiang, L.; Shu, C.; Wang, C. *Adv. Funct. Mater.* **2012**, *22*, 2187. (b) Lai, Y.-C.; Higashihara, T.; Hsu, J.-C.; Ueda, M.; Chen, W.-C. *Sol. Energy Mater. Sol. Cells* **2012**, *97*, 164.